Catalysis Today xxx (xxxx) xxx

Contents lists available at ScienceDirect

Catalysis Today

journal homepage: www.elsevier.com/locate/cattod

The synergy of catalysis and biotechnology as a tool to modulate the composition of biopolymers (polyhydroxyalkanoates) with lignocellulosic wastes

M. Ventura *, D. Puyol, J.A. Melero

Department of Chemical and Environmental Technology. ESCET, Universidad Rey Juan Carlos, 28933 Móstoles, Madrid, Spain

ARTICLE INFO

Keywords:
Photo-biorefinery
Heterogeneous catalysts
Polyhydroxyalkanoates
Integrated systems
Synergy

ABSTRACT

An integrated method coupling of heterogeneous and biological catalysis has proven effective for producing biopolymers using lignocellulosic urban solid waste as feedstock. Catalysts based on cheap and earth-abundant metals, such as Fe, Mg, Ca, or Zr with basic or acid properties, were used in the pre-treatment step, and phototrophic mixed cultures were chosen for the biological step. By changing catalysts composition, reaction temperature, and catalysts loading, high performance of the catalysts was achieved under the more optimal pretreatment of lignocellulose waste, with a solid conversion up to 86%, enriching the solid phase in the lignin polymer. The biological conversion of the liquid effluent in a photobioreactor yielded high production of PHA (up to 36 wt% on a dry basis). The characteristics of the polymer were strongly dependent on liquid feed, the composition of which depended on the type of catalysts used in the previous step. A poof of the concept of a new biorefinery design has been presented in this work, showing that it is possible to enhance the advantages of two different disciplines, heterogeneous catalysis, and photoheterotrophic biotechnology.

1. Introduction

The depletion of fossil resources and the increase in the CO_2 atmospheric level have pushed the scientific community to look for alternative feedstock [1]. Biomass (i.e., any organic material that comes from plants and animals) is one of the most promising feedstocks to replace fossil resources due to its availability in terms of quantity and because its renewable basis [2], making thus the natural replacement for fossil fuels for the generation of chemical products. Among all available biomass, biowastes should be considered a priority to be used as a source of chemicals, thus allowing for the best implementation of the circular economy [3,4]. Unlike fossil fuel feeds, biowastes feedstocks (e.g., municipal urban wastes (MUW), industrial effluents, or lignocelluloses) are highly complex, composed of a mixture of a large variety of compounds such as oxygenated chemicals and/or polymers, are very reactive, and chemically complex. About 2.01 billion metric tons of municipal solid waste are produced annually worldwide and are estimated to increase to 3.40 billion metric tons by 2050. An estimated 13.5% of today's waste is recycled, and 5.5% is composted, but between one-third and 40% of waste generated worldwide is not appropriately managed and instead dumped or openly burned. This MUW comprises a complex mixture of plastic residues, food, and lignocellulose wastes, where the latest accounts for about 22–66% of it [5]. Lignocelluloses are composed of mainly three components, cellulose (40–50%), hemicellulose (25–35%), and lignin (15–20%), being the almost perfect mixture for the generation of a wide variety of chemicals that could replace those coming from fossil resources [6]. However, transformations difficulties such as low selectivity on the final products are usually associated with their complexity [7]. As a result, new processes, reaction conditions, and catalytic materials need to develop to transition from fossil to biowastes feedstocks. Any biomass conversion process must be flexible enough to adapt to the evolving needs of the chemical industry, and in this regard, the requisite flexibility might be achieved by using a methodology that couples both chemical and biological approaches [8].

Concerning chemical catalysis, many approaches have been recently developed to efficiently transform biomass into high-added-value products [9–12], largely covered by homogeneous catalysis, transforming the more complex biomass: the biowastes. In this way, acids and bases were used to perform the depolymerization of cellulose and lignocellulose materials getting liquid effluents with a complex composition, not able to be transformed into high-added-value products suffering as well of problems of product separation, reactor corrosion,

* Corresponding author.
E-mail address: maria.ventura@urjc.es (M. Ventura).

https://doi.org/10.1016/j.cattod.2021.09.032
Received 15 April 2021; Received in revised form 10 August 2021; Accepted 23 September 2021
Available online 28 September 2021

poor catalyst recyclability, and the need for treatment of waste effluent [13]. Heterogeneous catalysts have the potential to overcome some of these limitations, such as catalyst separation and recyclability [14,15].

On the other hand, biological transformations have also been extensively used to treat biowastes, being the biosynthesis of storage bacterial compounds a valuable technology for making platform chemicals or high-added-value products [16,17]. In this context, Purple Phototrophic Bacteria (PPB) are microorganisms that can grow under a highly variable environment, including temperatures ranging from 0° to 37 °C, using light as the energy source and a wide range of organic and inorganic compounds as electron donors and acceptors. PPB can intracellularly store polyhydroxyalkanoates (PHA) due to light stress, nutrient imbalance, or carbon excess [18,19]. PHA is a family of bioplastic used for packaging or medical and pharmaceutical applications. A wide range of microorganisms can degrade PHA when needed by expressing intracellular or extracellular depolymerase enzymes, making PHA degradable in practically all biologically active environments, including soil, rivers, oceans, or sewage [20].

Previous works reported high PHA accumulation using a mixed culture of PPB, from 10% to 30% (cell dry basis), but the liquid feed composition highly influences this production [18,21]. In this regard, a pre-treatment of the feedstock allows the solubilization of the proper organic material and generates a liquid effluent that acts as feed liquor. Coupling heterogeneous catalysis for the pre-treatment of the lignocellulose material and PPB to produce PHA is an effective strategy to overcome the limitations of both techniques enhancing at the same time their strengths. Recent examples combining biological and catalytic technologies have been published, coupling a fermentation step with a chemocatalysis [22,23], even the drawbacks of fermentation, such as the low hydrolysis rate and the high cost associated with the reactor maintenance, and the need for a pre-treatment step [24–26]. Nevertheless, there are no examples of coupling heterogeneous catalysts and PPB. Most of the joint examples found in the literature set the biological treatment as the first step followed by the catalysis step. We pioneer in this work the development of the inverse approach for the treatment of urban lignocellulosic waste material: first, a lignocellulose heterogeneous catalytic pre-treatment by using Fe-based catalysts, followed by a biological treatment with a mixed culture of PPB in phototrophic anaerobic conditions. Catalytic lignocellulose pre-treatment usually gives a very complex liquid phase difficult to valorize but not for PPB, which can assimilate this complex mixture and accumulate a high-added-value product, PHA. The potential of this new platform is tested by quantitative assessment of the conversion of the waste organic matter into PHA.

2. Experimental

2.1. Source of lignocellulosic waste

Urban lignocellulosic waste was collected from an urban waste treatment facility located in Madrid (Spain), mainly composed of prune and gardening residues. The biowaste was blended and homogenized with a blade mill and screened to achieve less than 10 mm particle size previous to the catalytic pre-treatment.

2.2. Chemicals

For the analysis, glucose (99.99%), galactose (99.99%), mannose (99.99%), fructose (99.99%), xylose (99.99%), arabinose (99.99%), non-volatile acid standard mix (NVFA) (≥99.99%), volatile free acid mix (VFA) (≥99.99%), were purchased from Sigma-Aldrich, Spain, and used as received. Water (Milli-Q quality, Millipore, Spain) was used as a solvent. Mixed oxides were prepared by using the proper metallic precursor purchased from Sigma-Aldrich, Spain: $Fe(NO_3)_2.9H_2O$ (≥99%), ZrO_2 nanopowder(≥99%), NH_4VO_3 (≥99.9%), $Ca(NO_3)_2.4H_2O$ (≥99%), $Mg(NO_3)_2.6H_2O$ (≥99.99%) and an aqueous solution of NaOH (98%) in milli-Q water.

Table 1
Chemical composition of milled-treated feedstock (on dry weight basis).

Entry	Parameter	Value
1	TS (g/Kg)	980 ± 8
2	VS (% TS)	94 ± 1
3	COD (g Kg^{-1} TS^{-1})	1120 ± 40
4	Carbon (wt%)[a]	47.2 ± 0.1
5	Nitrogen	0.8 ± 0.2
6	Hydrogen	5.9 ± 0.4
7	Oxygen[b]	45.9
8	Cellulose (%)[c]	41.2
9	Hemicellulose	26.5
10	Lignin	24.8
11	Ash	0.5
12	CrI (%)[d]	68

[a] Determined by elemental analysis;
[b] calculated by the difference from the other elements;
[c] calculated from TGA analysis;
[d] Crystallinity index determined by XRD analysis.

2.3. Catalyst preparation

Iron mixed oxides were prepared by a co-precipitation method. We started from two different solutions, solution A, containing the metallic species in the desired concentrations, and solution B, containing the basic solution in a concentration of 2 M. At room temperature, these two solutions were added at the same rate to an empty flask with a stirring speed of 500 rpm until pH reached a value ≥ 10. Next, the precipitates were aged for 18 h at 80 °C in an oven. After that, the solids were washed with deionized water until pH≤ 7.5 and calcined, before their use in the catalytic experiments, at 550 °C for 4 h with a temperature rate of 2 °C/min. Finally, the solids were cooling down for 8 h to r.t.

2.4. Catalyst characterization

Metal content was determined by inductively coupled plasma (ICP-AES) with a Varian 715-ES ICP-Optical emission spectrometer after dissolving the solid in an HNO_3 aqueous solution. Phase purity was determined by X-ray diffraction (XRD) in A X′Pert PRO diffractometer (Malvern Panalytical, Netherlands), with θ / 2θ geometry, using Cu-Kα radiation. The data were collected from 5 to 90º (2θ) with a resolution of 0.02º. Specific surface areas of the solid samples were calculated by applying the BET method to the 77 K N_2 adsorption isotherms obtained in a Micromeritics Flowsorb apparatus (Micromeritics, Barcelona, Spain). Analysis of the composition of the fresh and catalytic treated lignocellulose residue was performed by thermogravimetric analysis (TGA) on a simultaneous TGA-DSC thermobalance (TGA-DCS1, Mettler-Toledo, S.A.E.) using a nitrogen flow rate of 100 mL/min and a heating rate of 10 °C/min.

2.5. Catalytic pre-treatment

Catalytic tests were performed in a 15 mL ace pressure tube equipped with a magnetic bar. Typically, 0.1 g of the lignocellulose material was mixed with a certain amount of catalyst (20 or 40 wt%) and then suspended in 5 mL of ultrapure water. The tube was then closed and heated to the desired temperature (120 or 140 °C). Stirring was stopped at fixed time intervals, and liquid samples (0.5 mL) were withdrawn and then analyzed by HPLC by following product evolution. The recycling tests were performed at the end of the reaction, using the desired catalysts under the fixed optimal conditions. The solid mixture, composed of the non-reacted solid lignocellulose and the catalyst, was separated from the aqueous phase by filtration, but after centrifugation of the reaction mixture. After filtration, the solid mixture was washed three times with water until no organic matter was detected in the liquid, then was dried

Table 2
Textural and chemical composition of Fe-based materials.

Sample	Molar ratio[a]	Mixed oxide structure	S_{BET} (m^2/g)
1Zr:0.25Fe	1:0.24	$ZrO_2{\cdot}(Fe_2O_3)_{0.12}$	95
1Zr:0.5 Fe	1:0.56	$ZrO_2{\cdot}(Fe_2O_3)_{0.28}$	82
1Zr:1Fe	1:1.1	$ZrO_2{\cdot}(Fe_2O_3)_{0.55}$	78
$MgCaO_2$	1Mg:1Ca	$MgCaO_2$	5
Fe/ $MgCaO_2$	0.2Fe:1Mg:1.2Ca	$(Fe_2O_3)_{0.1}$/ $MgCa_{1.2}O_2$	6
Fe-V/ $MgCaO_2$	0.2Fe:0.2 V:1Mg:1Ca	$(Fe_2O_3)_{0.1}(V_2O_5)_{0.1}$/ $MgCaO_2$	3

[a] Determined by ICP

Table 3
Crystallite size of the synthesized solids.

Entry	Solid	Cristal size (nm)
1	Zr:Fe	63
2	Zr:0.5Fe	65
3	Zr:0.25Fe	64
4	$MgCaO_2$	164
5	Fe-$MgCaO_2$	45
6	Fe-V/$MgCaO_2$	27

at 100 °C for 5 h, and catalyst and lignocellulose were separated through a sieve. The catalyst was then calcined at 550 °C to clean the surface of the eventual organic matter attached to the solid and finally reused in a new catalytic experiment. The catalyst was weighed after reaction and after purification and separation steps to determine the catalyst recovery shown in Table 4. Catalysts recovery was calculated as the difference between the initial amount of solid and the final solid weighed.

2.6. Photo-heterotrophic polyhydroxyalkanoate production

The activity of the phototrophic biomass on the liquid phase resulted from the catalytic pre-treatment was determined by Specific Phototrophic Activity (SPA) batch tests following the indications elsewhere [19]. In summary, triplicate experiments were performed in 160 mL anaerobic serum bottles (100 mL working volume) in a temperature-controlled incubator (at 30 °C) with an initial pH of 6.5. The incubator was illuminated with IR lamps (Philips BR125 IR, Spain) at around 45 W m^{-2} and covered with a UV/VIS filtering foil. An active mixed culture of PPBs was used as inoculum for the experiments. The phototrophic biomass was collected from a photo-anaerobic membrane bioreactor (PAnMBR) described in the literature [27]. The liquid phase from catalytic pre-treatment was used as the organic substrate to fix a concentration of 0.25–0.30 gCOD L^{-1}. The biomass samples for PHA measurements were extracted when the cultures reached the stationary stage. It is known that PHA accumulation is linked to organic substrate assimilation, which means it is associated with growth. A maximum of PHA accumulation is therefore expected before reaching the stationary stage [28].

2.7. Analytical Methods

Analytical determination of pH, total and volatile solids (TS, VS), total and volatile suspended solids (TSS, VSS), TKN, and COD of the solid and liquid fraction were carried out following Standard Methods for the Examination of Water and Wastewater. NH_4^+, PO_4^{3-} and total phosphorus (TP) were measured with Merck kits (Merck, Darmstadt, Germany). Elemental analysis (C, H, N, and S) of the solid fraction was performed by an elemental analyzer (Vario EL III, Elemental Analysis System GMHB, Germany).

Liquid samples were filtered through a cellulose-ester filter of 0.45 μm of pore size before the analysis (Advantech, Japan). VFA and NVFA were analyzed using an ion-exclusion Rezex™ ROA-Organic Acid H^+, while sugars and oligomers were analyzed using an ion-exclusion RPM-Monosaccharide Pb^{+2} (8%), both HPLC columns (Phenomenex, USA), coupled to a refractive index detector (Agilent, USA) and operated at 65 °C and 1 mL/min, with 0.005 M H_2SO_4 as the eluent for analysis of VFA and NVFA and at 85 °C and 0.8 mL/min, with ultrapure Milli-Q water as eluent for sugars and oligomers.

2.7.1. PHA measurement

After the photo-heterotrophic step, biomass samples were extracted at the fixed time intervals, fixed first with formaldehyde, centrifugated and filtered following by a lyophilization step to prevent PHA decomposition. PHA was extracted from the lyophilized- biomass by acid treatment and methanolysis reaction to generate their corresponding methyl ester, easily detected by GC. PHA production yield (Y_{PHA}, expressed as wt% on a dry basis of photo-heterotrophic biomass) was analyzed by gas-chromatography coupled to an FID detector, using an HP-5 Agilent column with a specific protocol previously described and calculated as Eq. (1) [19]:

$$Yield \quad PHA = \frac{mg \quad PHA}{mg \quad bacterial \quad biomass} \times 100 \tag{1}$$

Identification of the PHA monomers distribution was performed by direct aqueous-injection gas-chromatography coupled to a mass detector (320 GC-MS) using a Restek column Rxi-5Sil MS (30 m x 0.25 mm, 0.25 μm). This specific column for aqueous samples was initially maintained at 50 °C for 3 min, heated to 180 °C at 12 °C/min, and maintained for 5 min at 250 °C (7 °C/min). The injector was held at 320 °C, and He (1 mL/min) was used as the carrier gas.

The conversion of lignocellulose was calculated by the difference in solid weight before and after the reaction [29]. The concentrations of each product were calculated from their respective pre-calibrated plots of peak area versus concentrations for standard samples. The molar product distribution was calculated for each compound as Eq. (2):

$$Product \quad \boldsymbol{a} \quad distribution = \frac{[compound \quad a]}{\sum[total \quad compounds \quad of \quad the \quad mixture]} \times 100 \tag{2}$$

Table 4
Catalytic activity of Fe-based mixed oxides in the lignocellulose pre-treatment.

Entry	Solid	Conversion (%)	[NVFA] (mol/L)	[VFA] (mol/L)	[Sugars] (mol/L)	[oligomers] (mol/L)	Catalysts recovery
1	1Zr:0.25Fe	51	12.5	4.7	0.7	8.5	92–98
2	1Zr:0.5 Fe	58	11.4	3.7	1.2	4.3	
3	1Zr:1Fe	61	10.2	1.1	1.2	5.9	
4	ZrO_2	41	4.6	3.1	0.01	11.5	98
5	$MgCaO_2$	65	5.1	26.5	0.9	5.9	72
6	Fe/ $MgCaO_2$	72	6.1	27.3	4.4	6.2	92–98
7	Fe-V/ $MgCaO_2$	68	8.6	45.7	3.2	7.5	
8	No catalyst	15	0.5	0.8	0.06	0.05	–

Reaction conditions: [lignocellulose] = 20 g/L, 0.02 g catalyst, 5 mL H_2O, temperature = 120 °C, reaction time = 120 min. Products were identified and quantified by HPLC.

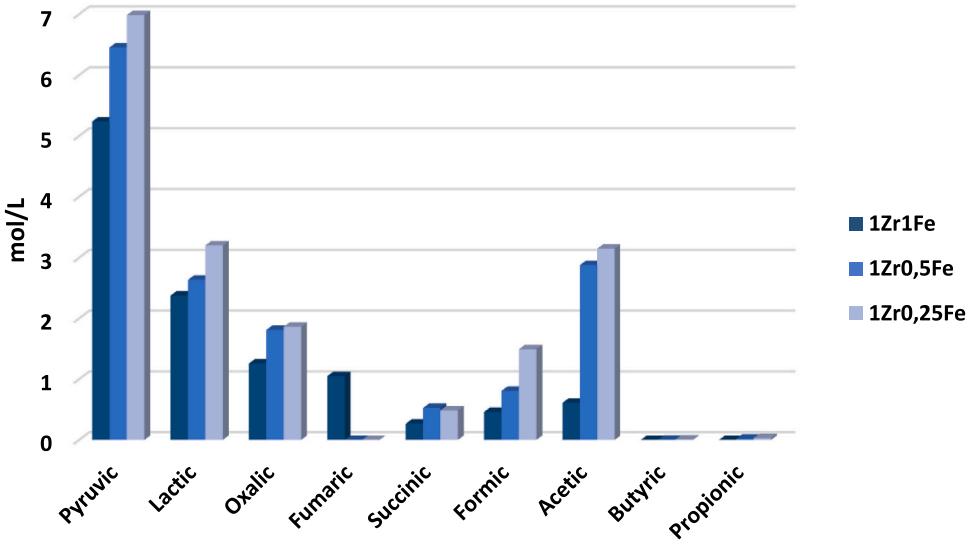

Fig. 1. Acids composition of the aqueous fraction when mixed oxides $ZrO_2{\cdot}Fe_2O_3$ were used for the lignocellulose catalytic pretreatment. Reaction conditions: [lignocellulose] = 20 g/L, 0.02 g catalyst, 5 mL H_2O, temperature = 120 °C, reaction time = 120 min.

3. Results and discussion

3.1. Lignocellulosic waste characterization

Chemical composition of this untreated, but milled sample was analyzed as described by NREL Laboratory Analytical Procedures, showing the results in Table 1 [30].

A solid with a high COD, suitable to be used as a feedstock in the process described here, was determined. Based on the elemental analysis, the residue has a low nitrogen content, which is critical in determining if nutrients from an external source such as NH4 + and PO43 are necessary for biological treatment. Because of the low N content detected, nutrients must be sourced externally. Concerning cellulose, hemicellulose, and lignin content, the residue has a high cellulose content, which difficult the pre-treatment step due to the low accessibility of cellulose [31].

The crystallinity index (CrI), determined by XRD, gives us an idea about the accessibility of the whole sample by the catalytic sites [19]. A high crystallinity hinders its accessibility hence its degradation. We observed moderate crystallinity derived from the mechanical treatment, which makes catalytic degradation easier [32].

3.2. Physicochemical characterization of catalysts

Fe was used as active metal because of its high potential to degrade cellulose [33]. It seems that the intimate contact of the cellulose fibers with Fe favors its degradation in water and at mild conditions. Therefore, the degradation by Fe could be extended to the reaction with a lignocellulose residue [34]. However, it should be accompanied by basic/acid support to enhance the hydrolysis rate of the carbohydrates (cellulose and hemicellulose) and to avoid the degradation of lignin that could yield polyphenolic compounds with potential toxicity for the next biological step, the treatment with PPB. To determine which one, acidity or basicity would be better to enhance the degradation rate of cellulose and hemicellulose, dismissing that of lignin, Fe was supported over acid (ZrO_2) or basic ($MgCaO_2$) solids. Vanadium was also supported together with Fe due to the enhanced cleavage rate of sugars, monomers, and oligomers, bserved by the mixture Fe–V, in other works [35].

Table 2 summarizes the main textural and physicochemical properties of Fe-based materials used in this work. ICP analysis confirms the molar composition of the synthesized solids according to the composition of the synthesis medium. The specific surface area (S_{BET}) for the Zr: Fe co-precipitated catalysts gradually decrease when Fe increase within the solid based on Zr. For these samples, an isotherm type IV is evidenced, corresponding to a mesoporous material. Solids based on $MgCaO_2$ presented lower specific surface area values with the same value for the three solids. In this case, these solids show type III isotherms. Isotherms are depicted in Fig. S1 of Supporting material. Because no differences were observed, only one isotherm of each group of solids, Zr:Fe, or based on MgCa, are shown in Fig. S1.

The XRD measurements characterized the crystalline structures of the mixed oxides after calcination. Their XRD patterns are shown in Fig. S2A, B. Concerning the solids composed of a mixture of Zr and Fe (Fig. S2A), and analyzing the crystallite size (Table 3, entries 1,2 and 3), there is no change in the value, meaning that just one phase was formed. In addition, a shift in the signal associated with 111 plane diffraction of ZrO_2 structure was observed, showing a possible inclusion of Fe atoms in the ZrO_2 structure.

A large number of peaks could be observed in the diffraction patterns that make difficult phase identification. However, peaks associated with α-Fe_2O_3 could be identified and peaks for monoclinic and cubic ZrO_2. It is well known that the assignment of cubic and tetragonal structures, based solely on the X-ray diffraction analysis, can be misleading because the cubic and tetragonal structures are very similar [36]. Nevertheless, a tetragonal structure can be distinguished from the cubic structure by the characteristic splitting of the diffraction peaks, whereas the cubic phase exhibits only single peaks. Splitting on the peaks was observed in the patterns, which led us to think that the tetragonal phase could also be present in these solids (Fig. S3). As is commented above, the identification of tetragonal phase just based on XRD analysis is often inaccurate [37,38], and even if the splitting was observed in the chromatograms, some diffraction peaks typical of a tetragonal phase did not appear; therefore, the assignation of the phases are of cubic and monoclinic, which are perfectly distinguished, leaving out the unclear tetragonal phase assignation.

The crystallite size was calculated using Scherrer's equation [36]. The average crystallite sizes of the monoclinic phase, calculated from the (111) diffraction peak, were 63 nm. Similarly, the average crystallite sizes, calculated from the (111) diffraction peak of the cubic phase, were 43 nm. Based on these observations and data reported in the literature, the Fe:Zr solids should be composed of a mixture of Brönsted and Lewis acid sites [39].

The XRD pattern of the solids based on $MgCaO_2$ is shown in Fig. S1B. Showing that the as-synthesized samples had the same diffraction planes

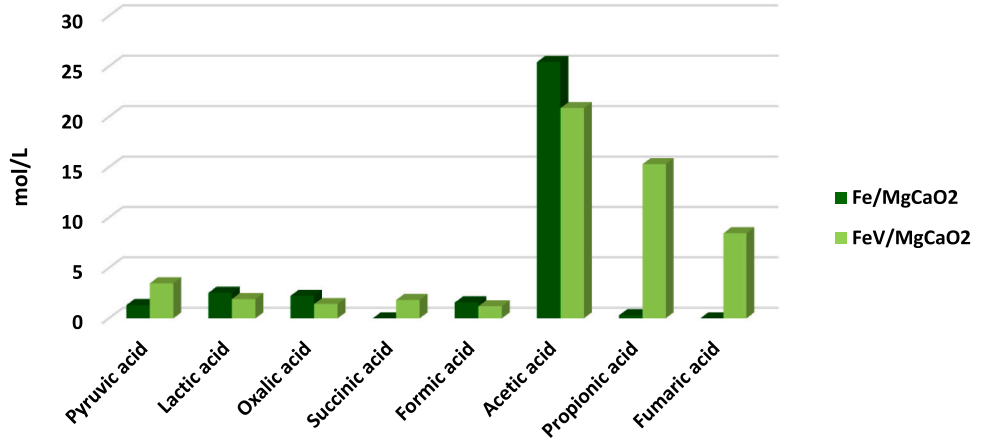

Fig. 2. VFA/NVFA composition of the liquid fraction when Fe_2O_3-V_2O_5/$MgCaO_2$ mixed oxides were used for the lignocellulose pretreatment. Reaction conditions: [lignocellulose] = 20 g/L, 0.02 g catalyst, 5 mL H_2O, temperature = 120 °C, reaction time = 120 min.

of MgO (periclase) and CaO but with shifts on its 2θ value, that means that a single phase of $MgCaO_2$ may form. Notably, the diffraction peak of the (220) face shifted with respect to pure MgO (2θ MgO_2 =62.2, 2θ this sample=62), which indicated a structural change of MgO by doping with Ca. In addition, some peaks associated with pure MgO_2 disappeared. Its crystallite size is much bigger than those of pure MgO, considering the bigger atomic radius of Ca^{2+}=1 Å than Mg^{2+}=0.72 Å makes sense that one single phase of $MgCaO_2$ was formed. Diffraction peaks of $MgCaO_2$ remained almost unaltered when Fe and V are supported into the surface. However, a significant change in the crystallite size was observed, going from 164 nm for $MgCaO_2$ to 45 and 27 nm for Fe/$MgCaO_2$ and Fe–V/$MgCaO_2$. This pattern was likely due to the formation of more than one phase during the synthesis of the solid. Other peaks identified with Fe_2O_3 and V_2O_5 were found in the XRD patterns.

3.3. Catalytic performance in the lignocellulose pre-treatment

3.3.1. Catalyst screening

First, we tested all the synthesized catalysts in the catalytic pretreatment of lignocellulose waste to settle the specific catalytic requirement to degrade the carbohydrates to less complex molecules. Then, to minimize the generation of residues and the need for high energy requirements, water was used as the solvent working under mild reactions conditions, autogenous pressure, and temperature in the range of 120–140 °C.

Table 4 shows the catalytic performance of Fe-based mixed oxides under study in terms of solid conversion and concentration towards the different compounds. The NVFA are considered the long-medium-chain fatty acids with high boiling points, such as fumaric, succinic, and oxalic acid. On the other hand, the VFA are the short-chain fatty acids such as acetic, propionic, butyric, and valeric acids. This table also shows sugars (mainly glucose and xylose), and oligomers.

The reaction with the Fe_2O_3·ZrO_2–based mixed oxides catalysts in different proportions achieved moderate conversions and high molar production towards NVFA (from 10 to 12.5 mol/L). The mixture was composed mainly of pyruvic (HPyr), lactic (HLac) and acetic (HAc) acids in various proportions depending on the tested catalysts. As Fe proportion is decreased in the mixed solid, the mixture of acids in the mixture increases, being HPyr the primary compound in this mixture (Fig. 1). This change in selectivity could also be attributed to the change in the specific surface area evidenced by the catalysts as the Fe content decreases. An enhancement of the specific surface area favors the accessibility of the lignocellulosic waste to the catalytic sites, increasing the degradation of the waste and achieving a higher NVFA and VFA proportion in the liquid effluent. Some non-identified products appeared in a minor proportion, maybe coming from lignin degradation, and further investigations are currently ongoing. No leaching of metals from the catalysts was observed since almost a quantitative recovery was achieved for the three solids. Besides, ICP-AES analysis of the aqueous liquid phase confirmed the absence of metals. Finally, a reaction carried out using Fe-free ZrO_2 as catalyst (Table 4; entry 4) yielded lower productivity and conversion than those reactions performed with Fe-supported catalysts and with a low formation of AGVs. These catalytic results confirm the critical role of Fe species in the degradation of carbohydrates.

Basic $MgCaO_2$–based catalysts were also tested under the same reaction conditions as those used for Fe_2O_3·ZrO_2 acid catalysts. When the reaction was performed using $MgCaO_2$ (Table 4, entry 5), higher conversion and VFA were achieved compared to Fe_2O_3·ZrO_2 catalysts. This mixture could be more suitable to perform the next step with the PPB, but it was discarded due to the low catalyst recovery obtained, where leaching of 20% of Mg was detected. Therefore, and considering the better results achieved when Fe was used as the active metal, it was supported over $MgCaO_2$ with two objectives: first to increase the stability of the catalysts and second to keep the selectivity of VFA. The strategy fits with the expected results with an increase in the recovery of the catalyst keeping the selectivity towards VFA (Table 4; entry 6). Vanadium was incorporated into the solid to increase the depolymerization of hemicellulose and cellulose and generate an aqueous effluent richer in VFA/NVFA due to the good results achieved in previous works with the Fe/V mixture in the degradation of sugars and monomers towards succinic, oxalic, and formic acid [35]. In fact, when the reaction was carried out (Table 4; entry 7), higher production of VFA was reached with a minor proportion of sugars in the mixture because of their degradation to VFA. The composition of both reaction mixtures is shown in Fig. 2, where is observed an enhanced concentration of propionic (HPr) and fumaric acid (HFum) when the reaction was carried out using $(Fe_2O_3)_{0.1}(V_2O_5)_{0.1}$/ $MgCaO_2$ as a catalyst. Finally, the reaction without catalyst achieved a low solid conversion and the negligible formation of the degradation compounds, which evidences the crucial role of the catalysts in the pre-treatment.

3.3.2. Reaction conditions: Preliminary screening

Temperature and catalyst loading were studied to enhance conversion and production towards simple and highly biodegradable acids. In the light of the previous catalytic results achieved, ZrO_2·$(Fe_2O_3)_{0.12}$ and $(Fe_2O_3)_{0.1}(V_2O_5)_{0.1}$/ $MgCaO_2$ were chosen to study the reaction conditions further. Since one of the objectives of this work is to perform the reaction under mild conditions, the temperature was increased just to 140 °C. Catalytic results are depicted in Fig. S4 in Supporting information. The Zr/Fe catalyst showed similar catalytic behavior with the increasing temperature, and just a slight increase in the production of

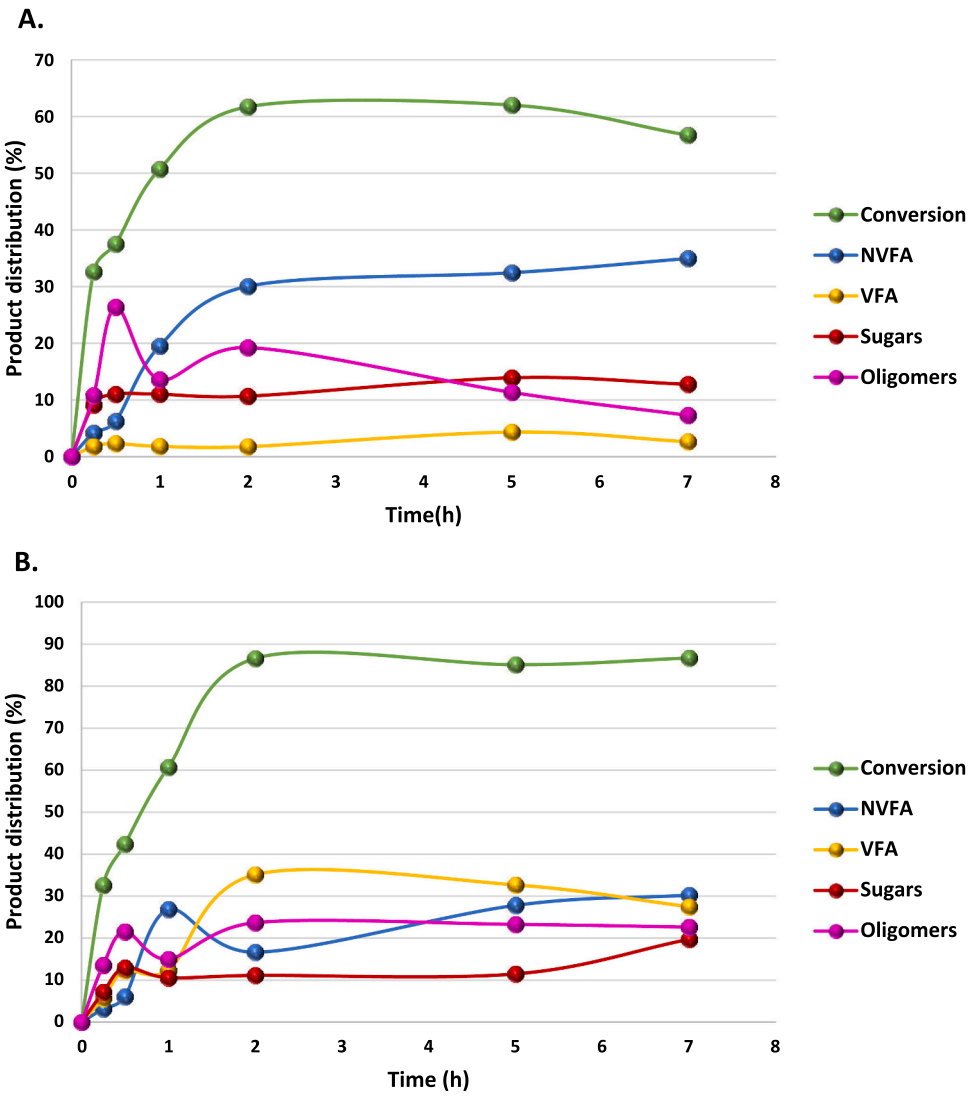

Fig. 3. Kinetics of the pre-treatment of lignocellulosic waste catalyzed by A. $ZrO_2{\cdot}(Fe_2O_3)_{0.12}$; B. $(Fe_2O_3)_{0.1}(V_2O_5)_{0.1}$/ $MgCaO_2$. Reaction conditions: [lignocellulose] = 20 g/L, 0.04 g catalyst, 5 mL H_2O, Temperature = A. 140 °C; B. 120 °C.

VFA was observed (Fig. S4A). In contrast, the Fe-V/$MgCaO_2$ catalysts (Fig. S4B) evidenced a clear decrease in the solid conversion when the reaction was carried out at 140 °C. This fact is likely due to the higher production of oligomers obtained with the increase of the temperature, which could partially block the active sites of the catalysts.

The catalyst loading effect for the two chosen catalysts was investigated under reaction temperatures of 140 °C for $ZrO_2{\cdot}(Fe_2O_3)_{0.12}$ and 120 °C for $(Fe_2O_3)_{0.1}(V_2O_5)_{0.1}$/ $MgCaO_2$ (Fig. S4). The catalyst loading did not affect the composition of the reaction mixture or conversion using Zr/Fe catalyst (Fig. S5A), but an increase in conversion and production of VFA was observed using Fe-V/$MgCaO_2$ (Fig. S5B). These catalytic data indicate the crucial role of the catalyst loading, which is strongly dependent on the catalyst features.

Further characterization of the remained solids was performed to investigate their degradation. TGA, COD, TS, and VS were determined after reaction and showed in Table S1. Derived from the pretreatment, solid with lower COD and TS were obtained being much lower as more effective was the pretreatment (with catalyst $(Fe_2O_3)_{0.1}(V_2O_5)_{0.1}$/ $MgCaO_2$), i.e. COD values decreased from 1120 to 827 and 421 g Kg^{-1}TS. TGA analysis of the solid after reaction with the two selected catalysts ($ZrO_2{\cdot}(Fe_2O_3)_{0.12}$ (identify as solid A); B. $(Fe_2O_3)_{0.1}(V_2O_5)_{0.1}$/ $MgCaO_2$ (identify as solid B)) were carried out (Figs. S6 and S7 respectively). These TGA analyses of the remaining solid after reaction were compared with the fresh lignocellulosic waste to monitor the degradation of the three polymers with the reaction time. The combination of these results indicates that cellulose and hemicellulose were degraded first during the catalytic reaction and a high % of lignin remained in the solid. This fact agrees with other authors [32] and agrees with the fiber structure; cellulose and hemicellulose are more accessible than lignin, and therefore easily degradable.

Some conclusions could be extracted from this analysis:

a) Higher degradation of cellulose was achieved using the solid $(Fe_2O_3)_{0.1}(V_2O_5)_{0.1}$/ $MgCaO_2$, due to the elevated proportion of lignin observed (55% vs 38% using $ZrO_2{\cdot}(Fe_2O_3)_{0.12}$). Complete degradation of hemicellulose was succeeded using both catalysts.
b) A kind of cellulose remained in both solids, should be a high crystalline cellulose and therefore less accessible to degrade. More investigations are currently performed in this sense.
c) Because of the high percentage of lignin, both solids, in particular solid B, could be valorized without posterior treatment step, as other authors described [40,41].
d) These findings corroborate the observed composition of the liquid phase, a low concentration of chemicals from the degradation of lignin was achieved.

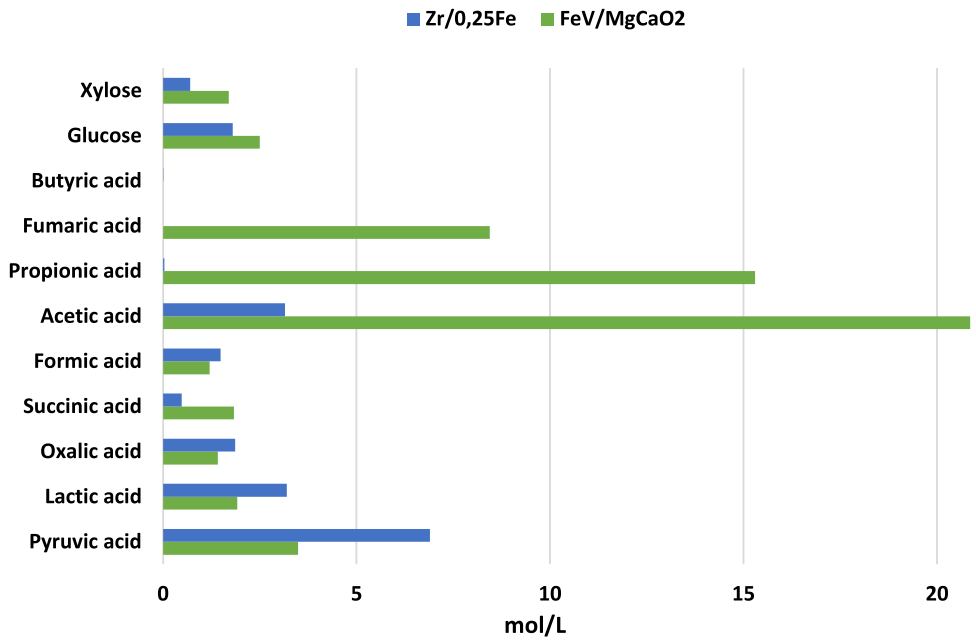

Fig. 4. Reaction mixture product distribution of NVFA, VFA and sugars for the pretreatment catalyzed by $ZrO_2{\cdot}(Fe_2O_3)_{0.12}$ or $(Fe_2O_3)_{0.1}(V_2O_5)_{0.1}/\ MgCaO_2$. Reaction conditions: [lignocellulose] = 20 g/L, 0.04 g catalyst, 5 mL H_2O, Temperature $ZrO_2{\cdot}(Fe_2O_3)_{0.12}$ = 140 °C; $(Fe_2O_3)_{0.1}(V_2O_5)_{0.1}/\ MgCaO_2$ = 120 °C, reaction time= 120 min.

Finally, reaction kinetics were carried out to gain some insights into the reaction time needed to degrade as much as cellulose and hemicellulose into NVFA or VFA (Fig. 3). As can be seen, maximum conversion and production to acids were achieved after 2 h of reaction, after that, some minor changes in the mixture composition were detected for both catalysts. After much time of reaction, 7 h, a decrease in the proportion of oligomers was detected, increased at the same time NVFA and sugars concentration for the reaction using $ZrO_2{\cdot}(Fe_2O_3)_{0.12}$ as catalyst (Fig. 3A). Regarding the reaction mixture coming from the catalytic treatment with $(Fe_2O_3)_{0.1}(V_2O_5)_{0.1}/\ MgCaO_2$ (Fig. 3B) a small decrease in sugar and NFVA concentration is noted at a long reaction time keeping the proportion of the other components. These changes were not big enough for considering 7 h, as optimal reaction time, given the unsustainable and unfriendly environmental factor of keeping a high temperature for such a high time. On the other hand, at shorter reaction times, 15 min, the conversion ratio is high for both catalysts. ca. 30% and 33%, which is mainly attributed to the depolymerization of hemicellulose and cellulose. When the quantity of oligomers is enough, they were converted into sugars, VFA, or NVFA depending on the catalyst used. This fact led us to think that depolymerization is highly influenced by the temperature while the transformation of these oligomers is principally modulated by the catalyst used.

It is important to note the different product distribution achieved by using both catalysts: $ZrO_2{\cdot}(Fe_2O_3)_{0.12}$ and $(Fe_2O_3)_{0.1}(V_2O_5)_{0.1}/\ MgCaO_2$, (Fig. 4) finding that an easily modulation of the mixture composition was possible by changing the kind of catalyst, being a key factor to obtain different polymers formulations as will be discussed in the biotechnology section.

Although it is not the objective of the study presented here, it is easy to note the different catalytic behavior of acid and basic catalysts. Catalysts with acid properties, those based on ZrO_2, drives the reaction to a mixture of NVFA being predominant HPyr and HLac. However, the catalysts with a basic character drive to VFA as the major products of the reaction mixture, composed mainly by HAc, HPr, even HFum was also obtained in a lower proportion. Further investigations are ongoing to correlate the features of catalytic sites with the degradation reaction mechanism.

3.4. Catalyst recyclability

One of the great advantages of the lignocellulose treatment process when carried out heterogeneously is its simple catalyst separation and reutilization, an essential requisite to make any process economically viable. The recyclability of the $ZrO_2{\cdot}(Fe_2O_3)_{0.12}$ and $Fe_2O_3)_{0.1}(V_2O_5)_{0.1}/\ MgCaO_2$ catalysts was evaluated by reusing in several catalytic cycles using the procedure described in the experimental section (Fig. 5).

Both catalysts shown a high stability after 4 consecutive runs. A slight decrease in the activity of the catalysts were observed during the first reuse in both cases keeping constant for the next successive runs. The reaction catalyzed by $ZrO_2{\cdot}(Fe_2O_3)_{0.12}$ shows a slight decrease on NVFA yield, but not big enough to be considered as a catalyst deactivation. However, higher decrease was detected for the reaction carried out with $(Fe_2O_3)_{0.1}(V_2O_5)_{0.1}/MgCaO_2$, fact that could be attributed to the small leaching of Mg observed in the liquid phase by ICP, detected by checking the solids after the first and the last (fourth) run. A mass drop of 2.6% (1st run) and 2.8% (4th run) was detected, meaning that the principal leaching of Mg species occurs in the first run with a practically negligible increase in the value after several reuses.

3.5. PHA accumulation: Phototrophic activity tests

The activity of the phototrophic biomass on the liquid phase coming from the catalytic pre-treatment was determined by Specific Phototrophic Activity (SPA) batch tests following the procedure elsewhere [42]. An active mixed culture of PPB was used as inoculum for the experiments. Parameters such as soluble COD (sCOD) and substrate consumption, biomass concentration and PHA yield were measured during the course of the activity test. PHA was analyzed at two points of the biomass growing to ensure the correct final time of the experiment corresponding with the maximum PHA accumulation.

Active biomass assimilated 83% and 66% of the sCOD in the $(Fe_2O_3)_{0.1}(V_2O_5)_{0.1}/\ MgCaO_2$ and $ZrO_2{\cdot}(Fe_2O_3)_{0.12}$ respectively (Fig. 6A) which was correlated with the biomass growth and concentration (Fig. 6B) 332 mg VSS L^{-1} and 289 mg $VSSL^{-1}$. Moderate consumption of the main nutrients (N and P) was detected, likely due to their high concentration compared to the organic carbon concentration

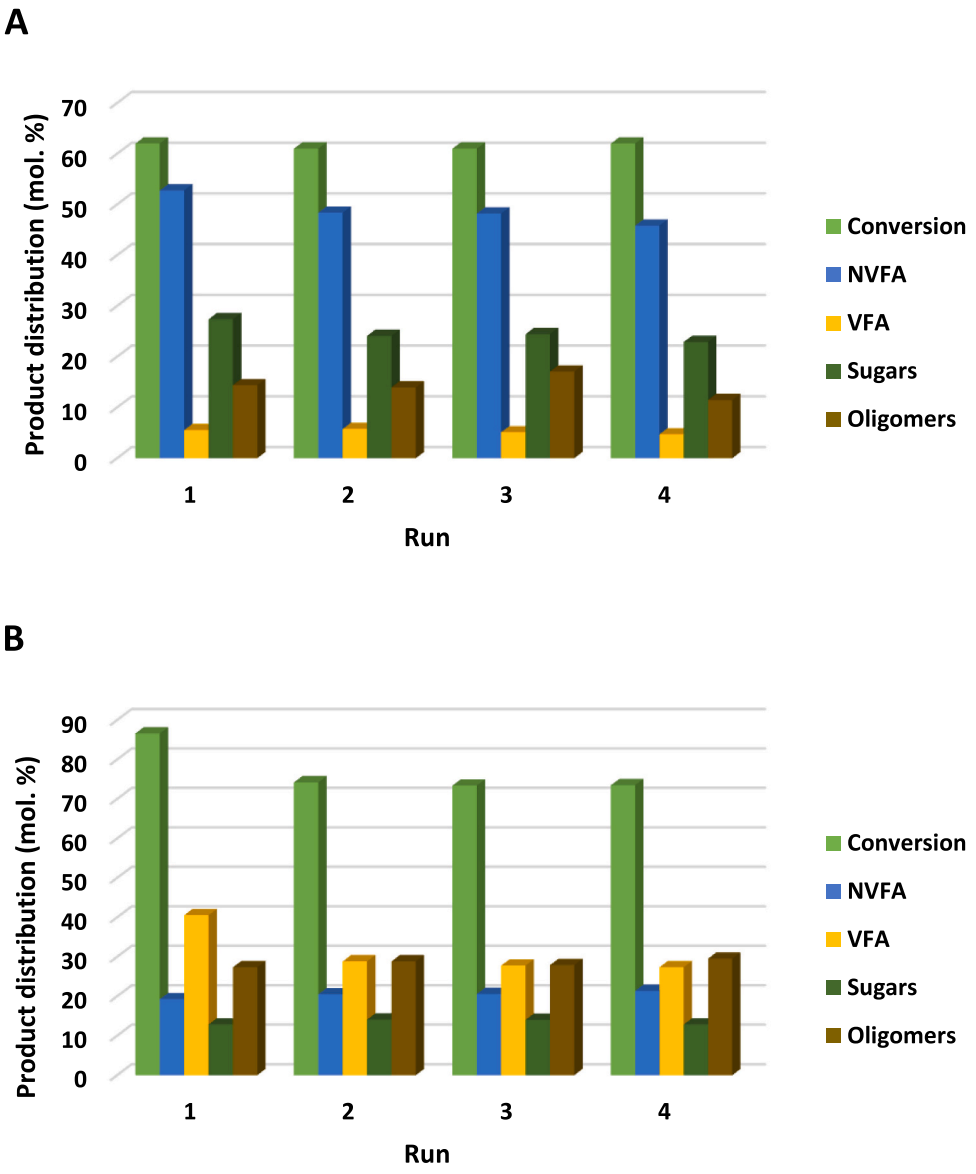

Fig. 5. Catalytic cycles of (A). $ZrO_2{\cdot}(Fe_2O_3)_{0.12}$; (B). $(Fe_2O_3)_{0.1}(V_2O_5)_{0.1}/MgCaO_2$ catalysts for lignocellulose pretreatment. Reaction conditions: [lignocellulose] = 20 g/L, 0.04 g catalyst, 5 mL H_2O, reaction time: 120 min. Temperature = A. 140 ºC; B. 120 ºC.

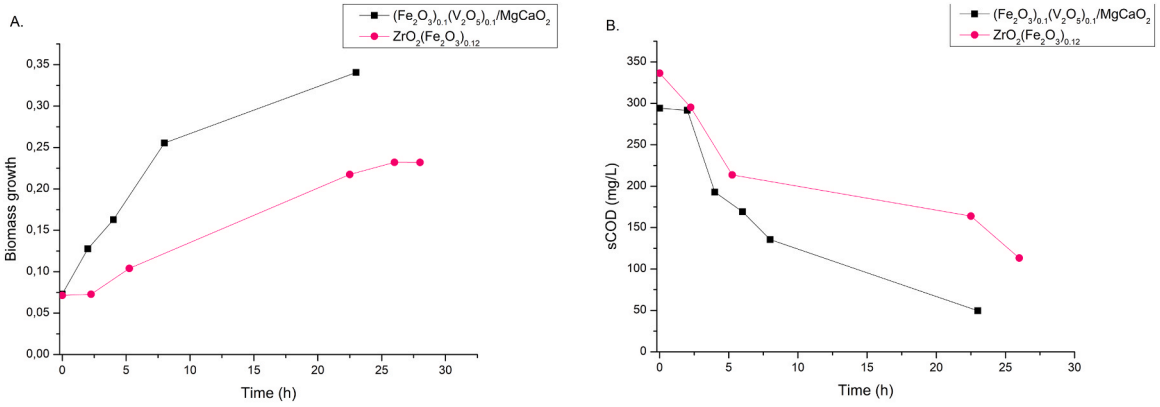

Fig. 6. A. Biomass growth expressed as gVSS $gSCOD^{-1}$ and B. sCOD consumption with the time. Black squares corresponds to the effluent obtained using $(Fe_2O_3)_{0.1}(V_2O_5)_{0.1}/ MgCaO_2$ as catalyst and pink circles using $ZrO_2{\cdot}(Fe_2O_3)_{0.12}$.

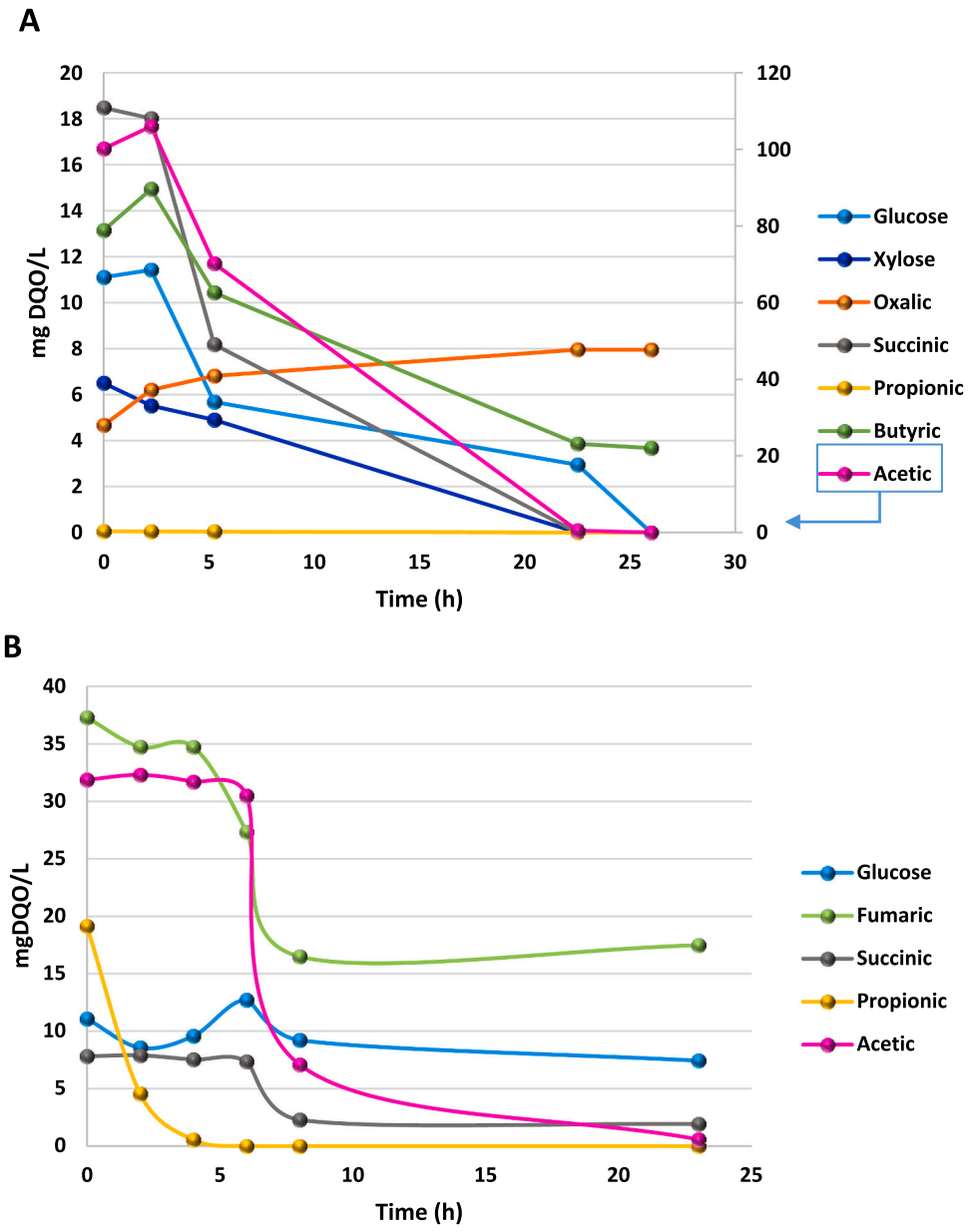

Fig. 7. Substrate distribution in the time course of the reaction using the liquid fraction coming from the reaction catalyzed by A. $ZrO_2{\cdot}(Fe_2O_3)_{0.12}$ and B. $(Fe_2O_3)_{0.1}(V_2O_5)_{0.1}$/ $MgCaO_2$.

(see Fig S8). In the light of these results can conclude that the hydrolysate was highly biodegradable by the mixed culture enriched in PPB microorganisms. However, the differences shown regarding each of the hydrolysates requires further analysis.

Substrate assimilation was followed in the time course of the reaction (Fig. 7). The reaction with the effluent generated with $ZrO_2{\cdot}(Fe_2O_3)_{0.12}$ (Fig. 7A) is composed mainly of HAc, HSucc, butyric acid (HBut), and glucose (Glu) but not all of them were consumed at the same rate. HSucc is the first substrate to assimilate following by HAc and HBut, fact that we expected because HSucc is a metabolite of the TCA cycle in the central metabolism of this kind of microorganism, therefore was assimilated easily than others [43]. HAc and HBut are the preferred substrate for growing and accumulate PHA[44]. The consumption of Oxalic acid (HOx) was practically negligible in the test, fact that we expected considering its low degradability in anerobic conditions, as has been observed by other authors achieving a low degradation rate of this acid working under the same conditions [45]. HBut was not completely assimilated, likely the microorganism had, at this point of the test, an over-reduction power, translated by NADH molecules, fact that enhance PHA accumulation. The other substrates are fully assimilated at the end of the test. Regarding the reaction using as liquid feed the effluent generated by $(Fe_2O_3)_{0.1}(V_2O_5)_{0.1}$/ $MgCaO_2$ (Fig. 7B) HFum, HAc and HPr are the major component in the mixture, observing the same fact than in Fig. 7A, HFum, which is one of the metabolites of TCA cycle, was assimilated firstly following than the preferred substrates, HAc and HPr. Although HFum was the first metabolite to assimilate, was not totally consumed, probably because there was a reductor excess in form of NADH that prevents its evolution into the Krebs cycle [46], this fact enhanced more the accumulation of PHA than the low degradation of HBut, as in the case of the liquid effluent coming from the reaction with $ZrO_2{\cdot}(Fe_2O_3)_{0.12}$, giving now higher values of total PHA. An interesting behavior is the prevalence of propionic acid assimilation during the first stage of the experiment. Indeed, propionic acid consumption prevented the assimilation of other VFAs, likely due to the activation of the propionyl-CoA pathway that competes with the acetyl-CoA pathway. This resulted in an inhibition of acetic, fumaric, and succinic acid

Table 5
Polymer yield using as liquid feed the liquid fraction coming from $ZrO_2{\cdot}(Fe_2O_3)_{0.12}$ and $(Fe_2O_3)_{0.1}(V_2O_5)_{0.1}$/ $MgCaO_2$.

Entry	Polymer	Acronym	Yield (wt% on dry basis)	
			$ZrO_2{\cdot}(Fe_2O_3)_{0.12}$	$(Fe_2O_3)_{0.1}$ $(V_2O_5)_{0.1}$/ $MgCaO_2$
1	Poly(3-hydroxypropionate)	P3HP	6	12.1
2	Poly(3-hydroxybutyrate)	P3HB	8.5	12.4
3	Poly(3-hydroxyvalerate)	P3HV	1.4	8.2
4	Poly(3-hydroxyhexanoate)	P3HH	4.6	3.6
		Total PHA	21	36

consumption. Once propionic acid was totally consumed, the acetyl-CoA pathway was re-activated and all the TCA metabolites were assimilated. Fact that has been previously observed for mixed cultures of purple phototrophic bacteria during the assimilation of a synthetic mixture of acetic, propionic, and butyric acids [47]. To our surprise, glucose in this case was barely assimilated, which may be cause of a redox disequilibrium that may affect the homeostasis and change the prevalence for organics accumulation.

t is worth noting that HPyr and HLac are not shown in this study because of the failure to identify them by HPLC, since they have the same retention times as EDTA and biotin, two macronutrients used in the Ormerod medium, having the same problem with oligomers. But, even so, an estimation of their consumption was performed (Fig S8A, B), in which oligomers were calculated by subtracting the sum of sugars and acids from the total sCOD. As can be seen, the more complex molecules, like the oligomers, remained at the end of the experiment, and their consumption rate was lower than the less complex substrates. The excess of reductants, caused by the presence of sugars and oligomers, may enhance the accumulation of the organic acids to accumulate PHA [46], as is furtherly detailed.

Different PHA composition was obtained derived from the two catalytic pre-treatment, which results in different PHA structures. Table 5 shows the characteristics of each PHA polymer, whereas Fig. 8 shows the

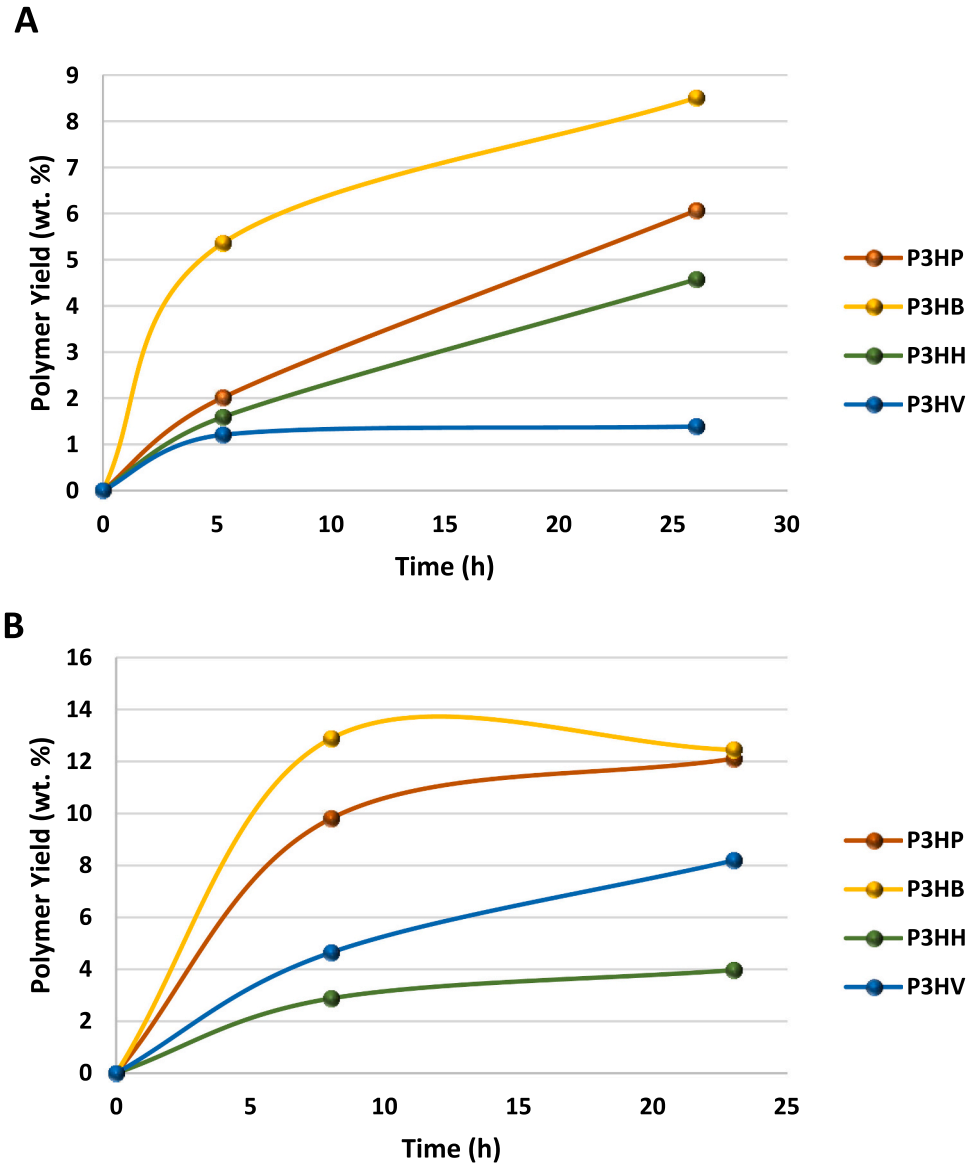

Fig. 8. Biopolymer yield evolution using the liquid fraction coming from the reaction catalyzed by A. $ZrO_2{\cdot}(Fe_2O_3)_{0.12}$ and B. $(Fe_2O_3)_{0.1}(V_2O_5)_{0.1}/MgCaO_2$. Monomers composition was determined by GC-MS.

time course of the PHA accumulation in the SPA tests. The polymer consists of a mixture of P3HP, PHB, PHV, and P3HH in different proportions, depending on the feeding liquid mixture. P3HB and P3HV have been thoroughly described in the literature as potential PHA obtained from PPB, and the metabolic mechanisms are clear [18]. These mechanisms include the direct conversion of the VFAs into acetyl Co-A that are further transformed into (R)-3-Hydroxybutyryl-CoA, which is then reduced to PHA by PHA synthase (PhaC). PHA can also produce by the reduction of other Acyl-CoA, e.g. from the degradation or synthesis of fatty acids, or even other pathways involving reductive processes concurring to PhaC [48]. However, the presence of P3HH and P3HP is noticeable and require an explanation. Medium-chain PHA like P3HH are usually produced by direct assimilation of medium-chain organic acids. For example, direct uptake of heptanoic acid by *Rhodospirillum rubrum* entails the polymerization of poly(3)-hydroxyheptanoate under excess of some reductants [49]. However, the conversion of short-chain organic acids like those appearing in our experiments to medium-chain PHAs like P3HH requires a previous step of chain elongation through the reverse β-oxidation process. This has been previously observed for chemotrophic PHA-producers [50], but up to the best of our knowledge, it has never been reported for PPB. Regarding P3HP, its production entails three potential metabolic pathways: (i) the propionaldehyde dehydrogenase route, (ii) the 3-hydroxypropionate route, and (iii) the malonyl-coenzyme A route [51]. In the same way, we were not able to find any instance showing the production of P3HP by a PPB culture (either pure or mixed cultures), and further analysis is therefore encouraged, which is out of scope from the present study.

Biopolymer, obtained by using the liquid effluent coming from the pre-treatment with $ZrO_2{\cdot}(Fe_2O_3)_{0.12}$, is composed mainly for P3HB, P3HP, and P3HH (41%, 29% and 22% respectively) and in a lower proportion PHV, 7%. However, the liquid feed getting from the pre-treatment with $(Fe_2O_3)_{0.1}(V_2O_5)_{0.1}$/ $MgCaO_2$ results in a very different biopolymer mixture: P3HP and P3HB are the main polymers in the mixture with similar proportions, 33% and 34%, and P3HV presents a non-discarded 22%. In this case, P3HH is the minor component with a 10%. As can be seen, the feed composition affects drastically the composition of the biopolymers, which leads us to think that an appropriate tuning on the catalyst properties will be a key parameter to obtain desired biopolymers thinking in a particular industrial application.

4. Conclusions

This work has shown, how the synergy of two different disciplines may be used to enhance the advantages of both. Catalysts based on earth-abundant and cheap metals have been used for the catalytic pre-treatment of an urban lignocellulose waste to yield a liquid effluent with an optimum composition for generating biopolymers (PHA based bioplastics) by a PPB-based biotechnology system. The catalysts showed good performance to depolymerize hemicellulose and cellulose, remaining a solid residue identified as a rich-lignin solid by-product. Recyclability, an important parameter taking into account for a potential industrial application, was also demonstrated for these catalysts, which keeping their activity for four consecutive catalytic runs. Features of the biopolymers accumulated in the microorganisms were strongly depending on the composition of the liquid effluent, highlighting the importance of a wise catalyst design to modulate the composition of this effluent. This work opens the door to a new integrated urban waste treatment combining heterogeneous catalysis and PPB photo-biorefineries. The proposed catalyst-PPB integrated biorefinery concept shown for the first time in this study has a strong potential and offers several new alternatives to develop new PHA formulations giving plenty of room for future research.

CRediT authorship contribution statement

M. Ventura: Conceptualization, Methodology, Validation, Investigation, Writing – original draft; **D. Puyol**: Methodology, Validation, Investigation, Writing – review & editing. **J. A. Melero**: Methodology, Writing – review & editing, Supervision.

Declaration of Competing Interest

The authors declare that they have no known competing financial interests or personal relationships that could have appeared to influence the work reported in this paper.

Acknowledgments

Financial support from the Regional Government of Madrid through the project S2018/EMT-4344 BIOTRES-CM is gratefully acknowledged. D. Puyol wishes to thank the Spanish Ministry of Economy for the Ramon y Cajal grant. This project has received funding from the European Union's Horizon 2020 research and innovation programme under the Marie Skłodowska-Curie grant agreement No 754382. The content of this article does not reflect the official opinion of the European Union. Responsibility for the information and views expressed herein lies entirely with the author(s).

Appendix A. Supporting information

Supplementary data associated with this article can be found in the online version at doi:10.1016/j.cattod.2021.09.032.

References

[1] R.P. Lee, Alternative carbon feedstock for the chemical industry? - Assessing the challenges posed by the human dimension in the carbon transition, J. Clean. Prod. 219 (2019) 786–796.
[2] J.C. Serrano-Ruiz, Biomass: a renewable source of fuels, chemicals and carbon materials, Molecules 25 (2020) 5217.
[3] P. Ghisellini, C. Cialani, S. Ulgiati, A review on circular economy: the expected transition to a balanced interplay of environmental and economic systems, J. Clean. Prod. 114 (2016) 11–32.
[4] C.A. De Mattos, T.L. De Albuquerque, Enabling factors and strategies for the transition toward a circular economy (CE, Sustainability 10 (2018) 4628, https://doi.org/10.3390/su10124628.
[5] F. Fava, G. Totaro, L. Diels, M. Reis, J. Duarte, O.B. Carioca, H.M. Poggi-Varaldo, B. S. Ferreira, Biowaste biorefinery in Europe: opportunities and research & development needs, N. Biotechnol. 32 (2015) 100–108.
[6] E.B. Vea, D. Romeo, M. Thomsen, Biowaste valorisation in a future circular bioeconomy, Procedia CIRP 69 (2018) 591–596.
[7] L. Capolupo, V. Faraco, Green methods of lignocellulose pretreatment for biorefinery development, Appl. Microbiol. Biotechnol. 100 (2016) 9451–9467.
[8] T.J. Schwartz, B.H. Shanks, J.A. Dumesic, Coupling chemical and biological catalysis: a flexible paradigm for producing biobased chemicals, Curr. Opin. Biotechnol. 38 (2016) 54–62.
[9] J.C. Serrano-Ruiz, R.M. West, J.A. Dumesic, Catalytic conversion of renewable biomass resources to fuels and chemicals, Annu. Rev. Chem. Biomol. Eng. 1 (2010) 79–100.
[10] A. Corma Canos, S. Iborra, A. Velty, Chemical routes for the transformation of biomass into chemicals, Chem. Rev. 107 (2007) 2411–2502.
[11] J.B. Binder, R.T. Raines, Simple chemical transformation of lignocellulosic biomass into furans for fuels and chemicals, J. Am. Chem. Soc. 131 (2009) 1979–1985.
[12] Z. Zhang, J. Song, B. Han, Catalytic transformation of lignocellulose into chemicals and fuel products in ionic liquids, Chem. Rev. 117 (2017) 6834–6880.
[13] H. Chen, J. Liu, X. Chang, D. Chen, Y. Xue, P. Liu, H. Lin, S. Han, A review on the pretreatment of lignocellulose for high-value chemicals, Fuel Process. Technol. 160 (2017) 196–206.
[14] Y.-B. Huang, Y. Fu, MicroRNA-100 inhibits osteosarcoma cell proliferation by targeting Cyr61, Tumour Biol. J. Int. Soc. Oncodev. Biol. Med. 35 (2014) 1095–1100.
[15] K. De Oliveira Vigier, F. Jérôme, Heterogeneously-catalyzed conversion of carbohydrates, Top. Curr. Chem. 295 (2010) 63–92.
[16] S.Y. Lee, Bacterial polyhydroxyalkanoates, Biotechnol. Bioeng. 49 (1996) 1–14.
[17] R.W. Lenz, Y.B. Kim, R.C. Fuller, Production of unusual bacterial polyesters by Pseudomonas oleovoransthrough cometabolism, FEMS Microbiol. Lett. 103 (1992) 207–214.

[18] J. Fradinho, L.D. Allegue, M. Ventura, J.A. Melero, M.A.M. Reis, D. Puyol, Up-scale challenges on biopolymer production from waste streams by purple phototrophic Bacteria mixed cultures: a critical review, Bioresour. Technol. 327 (2021), 124820.
[19] D.P. L. Diaz, M. Ventura,J.A. Melero, GCB Bioenergy 2020, accepted.
[20] D. Jendrossek, R. Handrick, Microbial degradation of polyhydroxyalkanoates, Annu. Rev. Microbiol. 56 (2002) 403–432.
[21] J.C. Fradinho, A. Oehmen, M.A.M. Reis, Photosynthetic mixed culture polyhydroxyalkanoate (PHA) production from individual and mixed volatile fatty acids (VFAs): substrate preferences and co-substrate uptake, J. Biotechnol. 185 (2014) 19–27.
[22] K.A. Goulas, F.D. Toste, Combining microbial production with chemical upgrading, Curr. Opin. Biotechnol. 38 (2016) 47–53.
[23] I. Wheeldon, P. Christopher, H. Blanch, Integration of heterogeneous and biochemical catalysis for production of fuels and chemicals from biomass, Curr. Opin. Biotechnol. 45 (2017) 127–135.
[24] Y. Sun, J. Cheng, Hydrolysis of lignocellulosic materials for ethanol production: a review, Bioresour. Technol. 83 (2002) 1–11.
[25] A.T.W.M. Hendriks, G. Zeeman, Pretreatments to enhance the digestibility of lignocellulosic biomass, Bioresour. Technol. 100 (2009) 10–18.
[26] B.C. Saha, Hemicellulose bioconversion, J. Ind. Microbiol. Biotechnol. 30 (2003) 279–291.
[27] I. de Las Heras, R. Molina, Y. Segura, T. Hülsen, M.C. Molina, N. Gonzalez-Benítez, J.A. Melero, A.F. Mohedano, F. Martínez, D. Puyol, Contamination of N-poor wastewater with emerging pollutants does not affect the performance of purple phototrophic bacteria and the subsequent resource recovery potential, J. Hazard. Mater. 385 (2020), 121617.
[28] J.C. Fradinho, A. Oehmen, M.A.M. Reis, Effect of dark/light periods on the polyhydroxyalkanoate production of a photosynthetic mixed culture, Bioresour. Technol. 148 (2013) 474–479.
[29] S. Sadula, N. Rodriguez Quiroz, A. Athaley, E.O. Ebikade, M. Ierapetritou, D. G. Vlachos, B. Saha, One-step lignocellulose depolymerization and saccharification to high sugar yield and less condensed isolated lignin, Green. Chem. 23 (2021) 1200–1211.
[30] J.B. Sluiter, R.O. Ruiz, C.J. Scarlata, A.D. Sluiter, D.W. Templeton, Compositional analysis of lignocellulosic feedstocks. 1. Review and description of methods, J. Agric. Food Chem. 58 (2010) 9043–9053.
[31] T.T. Teeri, Trends Biotechnol 15 (1997) 160–167.
[32] J. Zhang, A. Koubaa, D. Xing, H. Wang, Y. Wang, W. Liu, Z. Zhang, X. Wang, Q. Wang, Conversion of lignocellulose into biochar and furfural through boron complexation and esterification reactions, Bioresour. Technol. 312 (2020), 123586.
[33] W.A. Bell, J.M. Gibson, Degradation of cellulosic fibres in contact with rusting iron, Nature 180 (1957) 1065.
[34] Y. Feng, S. Long, X. Tang, Y. Sun, R. Luque, X. Zeng, L. Lin, Earth-abundant 3d-transition-metal catalysts for lignocellulosic biomass conversion, Chem. Soc. Rev. 50 (2021) 6042–6093, https://doi.org/10.1039/D0CS01601B.
[35] M. Ventura, D. Williamson, F. Lobefaro, M.D. Jones, D. Mattia, F. Nocito, M. Aresta, A. Dibenedetto, Sustainable synthesis of oxalic and succinic acid through aerobic oxidation of C6 polyols under mild conditions, ChemSusChem 11 (2018) 1073–1081.
[36] R. Srinivasan, R.J. De Angelis, G. Ice, B.H. Davis, Identification of tetragonal and cubic structures of zirconia using synchrotron x-radiation source, J. Mater. Res. 6 (1991) 1287–1292.
[37] C.V. Reddy, B. Babu, I.N. Reddy, J. Shim, Synthesis and characterization of pure tetragonal ZrO2 nanoparticles with enhanced photocatalytic activity, Ceram. Int. 44 (2018) 6940–6948.
[38] E.-M. Köck, M. Kogler, T. Götsch, L. Schlicker, M.F. Bekheet, A. Doran, A. Gurlo, B. Klötzer, B. Petermüller, D. Schildhammer, N. Yigit, S. Penner, Surface chemistry of pure tetragonal ZrO2 and gas-phase dependence of the tetragonal-to-monoclinic ZrO2 transformation, Dalton Trans. 46 (2017) 4554–4570.
[39] K. Tanabe, Surface and catalytic properties of ZrO2, Mater. Chem. Phys. 13 (1985) 347–364.
[40] M. Ventura, M.E. Domine, M. Chávez-Sifontes, Catalytic processes For Lignin Valorization into Fuels and Chemicals (Aromatics), Curr. Catal. 8 (2019) 20–40.
[41] F.G. Calvo-Flores, J.A. Dobado, Lignin as renewable raw material, Chem. Sus. Chem. 3 (2010) 1227–1235.
[42] D. Puyol, E.M. Barry, T. Hülsen, D.J. Batstone, A mechanistic model for anaerobic phototrophs in domestic wastewater applications: Photo-anaerobic model (PAnM), Water Res. 116 (2017) 241–253.
[43] G. Capson-Tojo, D.J. Batstone, M. Grassino, S.E. Vlaeminck, D. Puyol, W. Verstraete, R. Kleerebezem, A. Oehmen, A. Ghimire, I. Pikaar, J.M. Lema, T. Hülsen, Purple phototrophic bacteria for resource recovery: challenges and opportunities, Biotechnol. Adv. 43 (2020), 107567.
[44] J.C. Fradinho, A. Oehmen, M.A.M. Reis, Photosynthetic mixed culture polyhydroxyalkanoate (PHA) production from individual and mixed volatile fatty acids (VFAs): substrate preferences and co-substrate uptake, J. Biotechnol. 185 (2014) 19–27.
[45] S.L. Daniel, C. Pilsl, H.L. Drake, Anaerobic oxalate consumption by microorganisms in forest soils, Res. Microbiol. 158 (2007) 303–309.
[46] V. Montiel-Corona, G. Buitrón, Polyhydroxyalkanoates from organic waste streams using purple non-sulfur bacteria, Bioresour. Technol. 323 (2021), 124610.
[47] A. Alloul, S. Wuyts, S. Lebeer, S.E. Vlaeminck, Volatile fatty acids impacting phototrophic growth kinetics of purple bacteria: paving the way for protein production on fermented wastewater, Water Res. 152 (2019) 138–147.
[48] T. Tsuge, Metabolic improvements and use of inexpensive carbon sources in microbial production of polyhydroxyalkanoates, J. Biosci. Bioeng. 94 (2002) 579–584.
[49] H. Brandl, E.J. Knee, R.C. Fuller, R.A. Gross, R.W. Lenz, Ability of the phototrophic bacterium Rhodospirillum rubrum to produce various poly (β-hydroxyalkanoates): potential sources for biodegradable polyesters, Int. J. Biol. Macromol. 11 (1989) 49–55.
[50] S. Fiedler, A. Steinbüchel, B.H.A. Rehm, PhaG-mediated synthesis of Poly(3-hydroxyalkanoates) consisting of medium-chain-length constituents from nonrelated carbon sources in recombinant Pseudomonas fragi, Appl. Environ. Microbiol. 66 (2000) 2117–2124, 2117 LP – 2124.
[51] B. Andreeßen, N. Taylor, A. Steinbüchel, Poly(3-hydroxypropionate): a promising alternative to fossil fuel-based materials, Appl. Environ. Microbiol. 80 (2014) 6574–6582, 6574 LP – 6582.